JOURNAL OF MATERIALS SCIENCE 30 (1995) 1386–1390

Antiferroelectric lead zirconate thin films derived from acetate precursors

K. K. LI, F. WANG, G. H. HAERTLING
Department of Ceramic Engineering, Clemson University, Clemson, SC 29634, USA

Antiferroelectric lead zirconate ($PbZrO_3$) films derived from acetate precursors have been fabricated on Pt/Ti-coated silicon wafers and fused silica at 700 °C with an automatic dip-coating process. Films formed directly on the metallized silicon wafer showed the coexistence of perovskite and pyrochlore phases. A pre-coated titania layer of about 10 nm facilitated the formation of the desired perovskite phase. Films deposited on fused silica exhibited interactions between lead and silica which inhibited the crystallization of the films. In this case, a pre-coated titania layer in the range 50–75 nm acted as a diffusion barrier layer, allowing the formation of the perovskite phase. Antiferroelectricity in the films was confirmed by X-ray superstructure, dielectric double hysteresis loops and d.c. bias behaviour at room temperature. The corresponding transverse electro-optic properties were also measured for films deposited on fused silica.

1. Introduction

Lead zirconate (PZ) is a typical antiferroelectric (AFE) material at room temperature [1, 2], from which the ferroelectric (FE) state can be induced when subjected to a sufficiently large electric field. However, this transition field usually exceeds the material breakdown strength, and consequently, the field-enforced AFE → FE transition is usually carried out at a few degrees centigrade below its Curie point (~230 °C) [2]. Owing to the antiparallel arrangement of the spontaneous polarization directions, its unit cell is a superstructure of orthorhombic symmetry consisting of eight perovskite units [3, 4]. Although lead zirconate has been well studied in the bulk form, its thin-film properties have rarely been reported.

Preparation of the PZ films was first motivated by a mixed-phase problem encountered in the solution-derived FE lead zirconate titanate (PZT) or lanthanum-modified PZT (PLZT) thin films. The coexistence of the perovskite and the pyrochlore phases was commonly observed in these films [5–8] fabricated from different precursor systems, and the amount of the pyrochlore phase increased as the film composition approached the zirconium-rich side [5, 8]. Thus, PZ was expected to be the most difficult composition in the PZT family to obtain with the desired perovskite phase. Moreover, studying the formation of the PZ films benefits the overall knowledge about microstructure evolution mechanisms as well as providing a proper processing technique which could be applied to other PZT or PLZT compositions.

Remedies to the mixed-phase problem in the PLZT films have been proposed by forming a buffer layer of either lead titanate (PT) [9] or lanthanum-modified lead titanates (PLTs) [8] prior to the PLZT film deposition. These PT-based compositions were found to crystallize readily into the perovskite structure at lower temperatures, and PLZT films isostructurally grown on these buffer layers showed enhanced perovskite phase formation. Similar conclusions were noted for sol–gel $LiNbO_3$ films [10] in which the perovskite phase was formed at a much lower temperature when deposited on top of an existing perovskite layer.

AFE materials possess unique dielectric, piezoelectric [11, 12] and electro-optic properties [13] which make them suitable for devices such as micro-displacement transducers. Because PZ is the base composition for some AFE compounds [14], for example, tin-modified PZT, preparation of the PZ films provided a starting point for other PZ-based AFE films. Further incentive to prepare PZ films on transparent substrates resulted from the theoretical interest in studying the electro-optic behaviour associated with the field-induced AFE → FE phase transition [13].

The purpose of this work was to overview the processing aspects of the PZ films prepared from the acetate precursor system and to study their microstructure evolution. Preliminary results on the electric/dielectric and electro-optic properties of the AFE PZ films are also discussed.

2. Experimental procedure

The specific precursors used in the preparation of the PZ films and the TiO_2 pre-coats were previously reported in a paper describing the acetate solution system for PLZTs [15]. For the PZ composition, lead subacetate powder, $Pb(OOCCH_3)_2 \cdot 2Pb(OH)_2$, and aqueous zirconium acetate solution (ZAA) were used. The oxide contents of the precursors were assayed beforehand. Lead subacetate was first dissolved into

0022–2461

the ZAA and continuously stirred for 20 min. Methanol was then added into the mixture as a solvent and stirred for another 10 min. The final coating solutions contained 6–8.5 wt % oxide.

The TiO_2 pre-coats were derived from titanium diisopropoxide biacetylacetonate (TIAA), 75 wt % in isopropanol. It was mixed with methanol at a weight ratio of 1:5 to form the coating solution containing about 3 wt % TiO_2.

Films were deposited on Pt/Ti-coated silicon wafers and optically polished fused SiO_2 for measuring their dielectric and electro-optic properties, respectively; however, silver foils were also occasionally used as substrates. All films were formed by an automatic dip-coating process which involved a multiple dipping and firing approach [16]. Substrates were withdrawn from the solutions at a speed of 18.7 cm min^{-1}. The coating cycle was repeated 15–30 times which gave a final film thickness ranging from 0.6–1 μm. Each coating layer was fired at 700 °C for 2 min.

Pulverized solid samples obtained by drying the coating solution at 60 °C were subjected to thermogravimetry analysis (TGA) and differential thermal analysis (DTA) in air. The dried samples were also heated in a furnace at various temperatures for 1 h for X-ray diffraction (XRD) and other analyses.

Dielectric measurements were made at 1 kHz. Hysteresis loops were measured with a modified Sawyer–Tower circuit. The transverse electro-optic properties were measured by means of a phase-detection technique in the transmission mode [17]. Evaporated copper was used as the electrodes.

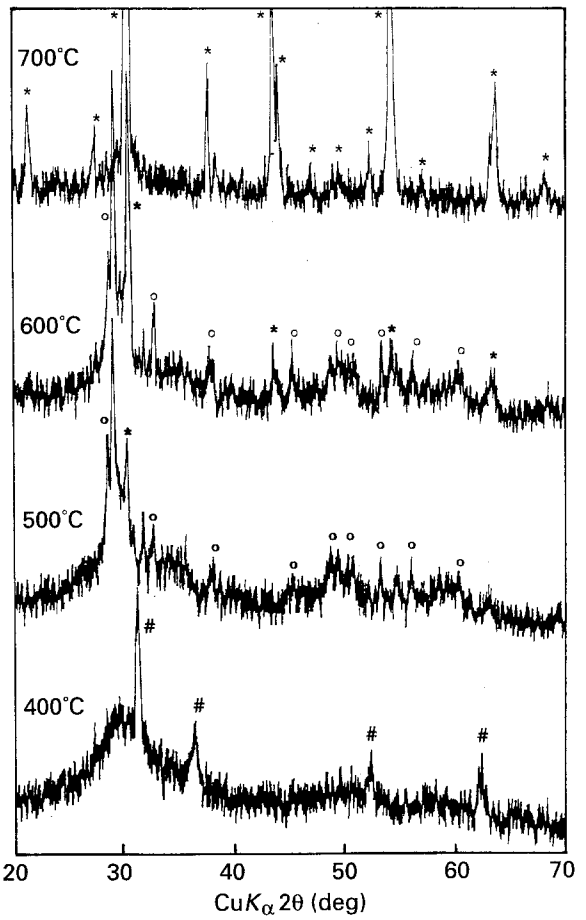

Figure 1 XRD patterns of dried powder pyrolysed at different temperatures. (#) Pb, (○) oxidized Pb, (*) perovskite $PbZrO_3$.

3. Results and discussion

3.1. Thermal decomposition and crystallization behaviour

XRD patterns of the pyrolyzed powder are shown in Fig. 1 as a function of the firing temperatures. Powders heated below 400 °C (not shown) had a very broad amorphous peak centred around ~30° 2θ (CuK_α). Metallic lead appeared at 400 °C, and was subsequently oxidized at higher temperatures. A small amount of the perovskite PZ phase started to form at 600 °C and became the only phase at 700 °C. Formation of metallic lead and PbO_x during the thermal decomposition process was not uncommon, for it has also been reported in sol–gel systems for PZT [18] and PZ [19]. The pyrochlore phase, however, was not appreciable in these XRD results.

Fig. 2 shows the TGA and DTA results of dried solid samples heated from room temperature to 800 °C at a rate of 10 °C min^{-1}. The sample lost about 30% of its weight during pyrolysis, and this corresponded to approximate 2 moles each of OAc^- and OH^- (or H_2O) per mole of PZ. By comparing the results with Fig. 1 and other infrared spectra data, the dried solid first underwent dehydroxylation (or dehydration) at temperatures below 200 °C. The endothermic peaks between 250 and 400 °C were attributed to the decomposition of the acetate group and possibly the melting of lead. The broad exothermic peak between 400 and 600 °C accompanied by about 5% weight loss was the oxidation of residual carbonaceous material and lead. The small exothermic peak at about 660 °C corresponded to the crystallization of the perovskite PZ. From these results it was decided to set the processing temperature for the PZ films at 700 °C.

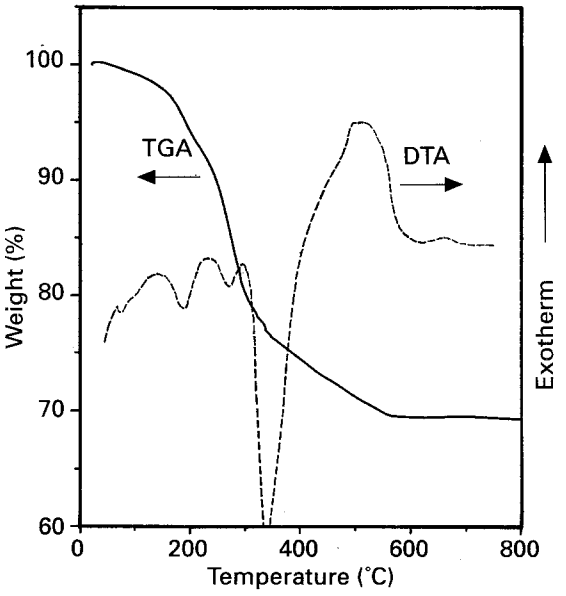

Figure 2 TGA and DTA curves of dried $PbZrO_3$ powder heated in air at a rate of 10 °C min^{-1}.

3.2. Film microstructure and phase formation

3.2.1. Pt/Ti-coated silicon substrates

Fig. 3 shows a scanning electron micrograph of a ten-layer PZ film deposited on the Pt/Ti-coated silicon substrate and treated afterwards with a dilute HF–HCl etching solution. The presence of two distinct phases in the film, also detected by XRD, was a phenomenon similar to that found in PLZT films [5–8]. The pyrochlore phase region appeared darker than the perovskite one, owing to their differences in lead content.

From Figs 1 and 2, the appearance of metallic lead during the decomposition process and the large temperature difference between the formation of lead (~375 °C) and the crystallization of the perovskite phase (~660 °C), suggests that: (1) the loss of lead and (2) segregation of the lead species during the firing process might be responsible for the observed microstructure. The absence of the pyrochlore phase in powdered samples indicated that the loss of lead was more significant in thin films. These arguments are also supported by the fact that a faster heating rate, which would shorten the time to reach the crystallization temperature, improves the film microstructure [5].

Using PT or PLT buffer layers proved to be as effective in modifying the microstructure of the PZ film as those of the PLZT films. However, a TiO_2 layer was also found to be capable of improving the perovskite phase formation. Results from XRD and TGA/DTA experiments on composition PT indicated that lead had a much greater tendency to combine with titanium; i.e. no lead was detected by XRD and perovskite PT could be formed at ~470 °C which was almost 200 °C lower than that of PZ. A relatively thin TiO_2 layer, dip-coated on to the Pt/Ti-coated silicon substrate and fired at 700 °C for 30 s, was estimated [16] to be in the region of 10 nm and possessed a rutile structure. The etched microstructure of a PZ film processed at the same conditions as in Fig. 3 but with a pre-coated TiO_2 layer is shown in Fig. 4. The pyrochlore phase was not discernible in this picture and the film morphology has been improved dramatically with the TiO_2 pre-coat. The reasons for the improved microstructure of the PZ films deposited with a TiO_2 pre-coat are presently under study.

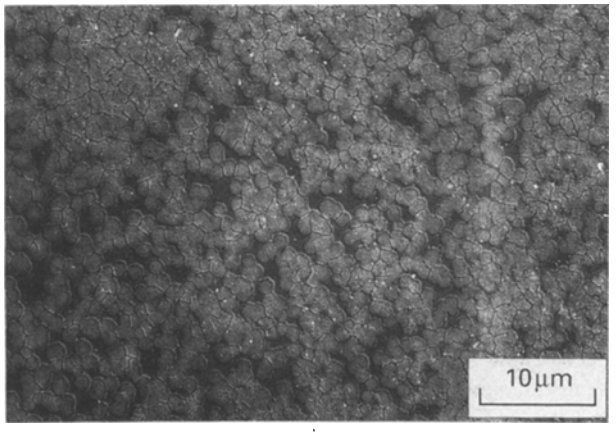

Figure 3 Scanning electron micrograph of a ten-layer $PbZrO_3$ film deposited on a Pt/Ti-coated silicon substrate.

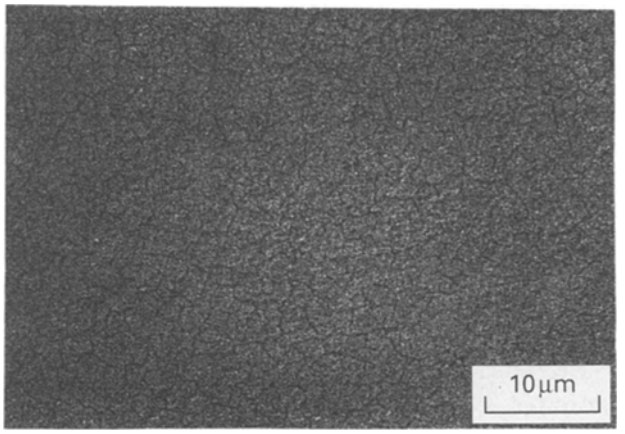

Figure 4 Scanning electron micrograph of a ten-layer $PbZrO_3$ film formed on a Pt/Ti-coated silicon substrate with a thin TiO_2 pre-coat.

For Pt/Ti-coated silicon substrates, growing films on PT or PLT layers was more easily controlled than on a TiO_2 layer. However, TiO_2 has proved to be very useful for films deposited on fused SiO_2 substrates. On both types of sublayers, however, the PZ films were found to retain a small amount of the pyrochlore phase when examined by XRD, therefore, excess lead (as much as 20 at %) has been added in the preparation of subsequent films in order to compensate for its loss.

3.2.2. Fused silica substrates

PZ films deposited directly on to fused SiO_2 substrates and fired at 600–700 °C were colourless and showed no crystallinity under XRD. Large cracks were presented throughout the films and also the substrate surfaces, suggesting a film–substrate interaction. Films could be crystallized into the perovskite structure with the PT or PLT buffer layers but regions of imperfections still could be found. This indicated that in these lead-containing layers, lead was responsible for the film–substrate interactions. This effect was not unexpected because it was well known that PbO reacts easily with SiO_2 to form low-melting silicates. The TiO_2 sublayer was found to be the better choice in this case, yet it required a layer thickness of 50–75 nm to inhibit such interactions. Similar uses of TiO_2 layers have been reported for PLZT films deposited on glass substrates [20] and in CMOS devices integrated with PLZT ferroelectrics [21].

The crystallized PZ films were transparent, light yellow in colour and suitable for transmission electro-optic properties measurements. Fig. 5 shows the morphology of a 1 μm PZ film deposited on a fused SiO_2 substrate pre-coated with a TiO_2 layer. It can be seen in its XRD pattern, Fig. 6, that this film was highly crystallized into a single perovskite phase. The superstructure orthorhombic {1 1 0} peak at about 16.9° 2θ confirmed the multiple-cell structure of this film.

3.2.3. Microcracks

All PZ films deposited on the above two types of substrate had a certain degree of microcracking as can

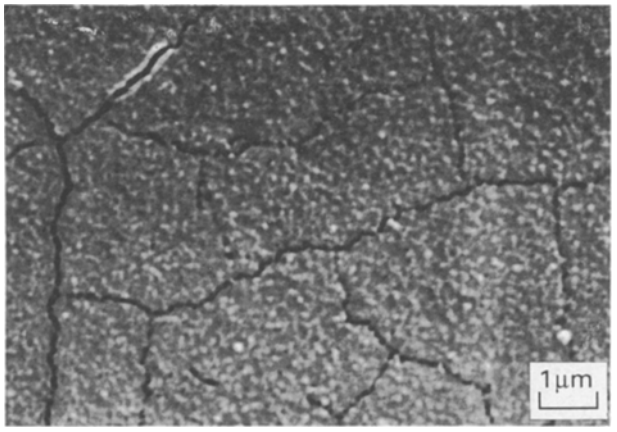

Figure 5 A 1 μm $PbZrO_3$ film formed on fused SiO_2 pre-coated with a TiO_2 layer.

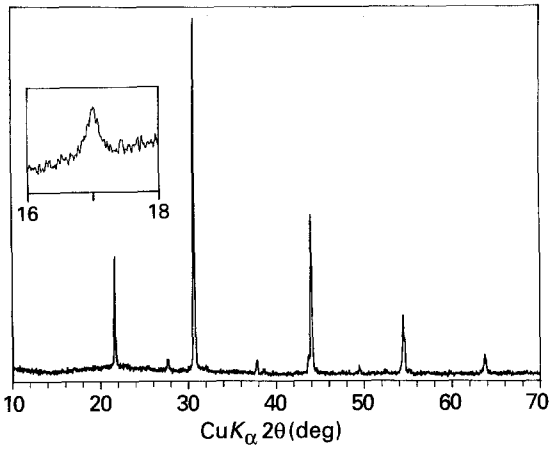

Figure 6 XRD pattern of the $PbZrO_3$ film shown in Fig. 5 and its superstructure peak characterizing the antiferroelectricity.

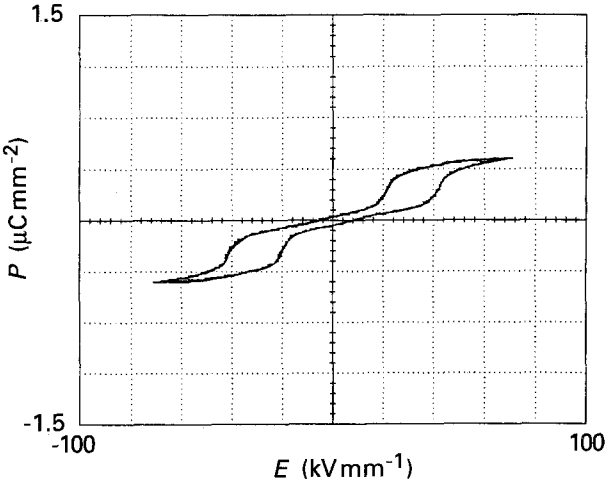

Figure 7 A typical dielectric double hysteresis loop of $PbZrO_3$ film deposited on Pt/Ti-coated silicon substrate with a TiO_2 layer.

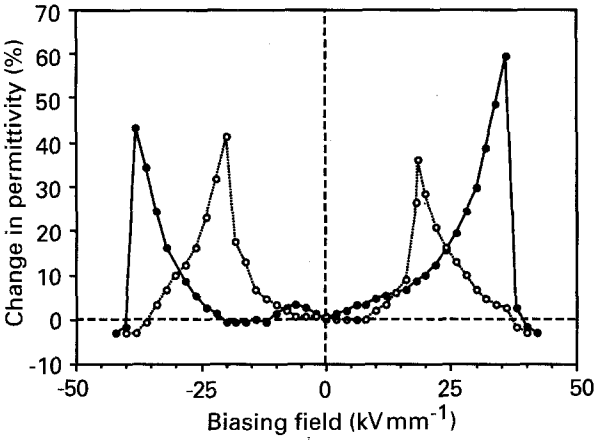

Figure 8 Variation of the $PbZrO_3$ film permittivity as a function of the d.c. bias. (●) Increasing bias, (○) decreasing bias.

be seen in Figs 3–5. While this phenomenon was not observed in other FE PLZT films deposited on the same substrates under similar processing conditions, their formation was attributed particularly to the extra volume shrinkage which occurred at the phase transition from the higher temperature paraelectric state to the lower temperature AFE state [14] during the film cooling stage. On the other hand, microcracks were not seen in PZ films deposited on substrates such as silver, which possessed a higher thermal expansion coefficient ($22 \times 10^{-6}\,°C^{-1}$) than those of the platinum silicon ($2.6 \times 10^{-6}\,°C^{-1}$) and fused SiO_2 ($0.5 \times 10^{-6}\,°C^{-1}$). Because the general PLZT films were in a compressive state when deposited on silver foils [22], it suggested that the microcracks could be avoided by a residual compressive stress. These microcracks, however, did not prevent the measurements of the electrical and optical properties, yet they affected somewhat the optical quality of the films on fused SiO_2.

3.3. Dielectric and electro-optic properties

All the PZ films had a dielectric constant at 1 kHz in the range 200–250. Dissipation factors were 0.02–0.03 and d.c. resistivities were greater than $10^{10}\,\Omega$cm. A typical polarization versus electric field (P–E) double hysteresis loop measured at room temperature is shown in Fig. 7 for a 0.8 μm PZ film deposited on a Pt/Ti-coated silicon substrate with a TiO_2 sublayer. The AFE→FE transition field was about $40\,kV\,mm^{-1}$ and the reverse FE→AFE was about $20\,kV\,mm^{-1}$. The FE phase saturated at about $60\,kV\,mm^{-1}$ with a polarization between 0.3 and $0.4\,\mu C\,mm^{-2}$.

The success in observing the double hysteresis loop of PZ film at room temperature was attributed to the superior dielectric strength usually found for thin-film materials. For example, the AFE→FE transition field found for these PZ films was an order of magnitude greater than the reported values for bulk materials [2]. Such a large field would certainly cause breakdown in bulk PZ.

Inasmuch as the slope of the P–E hysteresis loop indicates the permittivity of the sample, this parameter would be expected to increase sharply as the sample passed through the AFE→FE and FE→AFE phase transitions. Fig. 8 shows the variation of the permittivity of a virgin PZ film recorded as a function of a slowly varying d.c. bias applied first in the positive direction. The permittivity sharply increased by 40%–60% of its original value at the AFE→FE transition field and dropped as the loop saturated. The

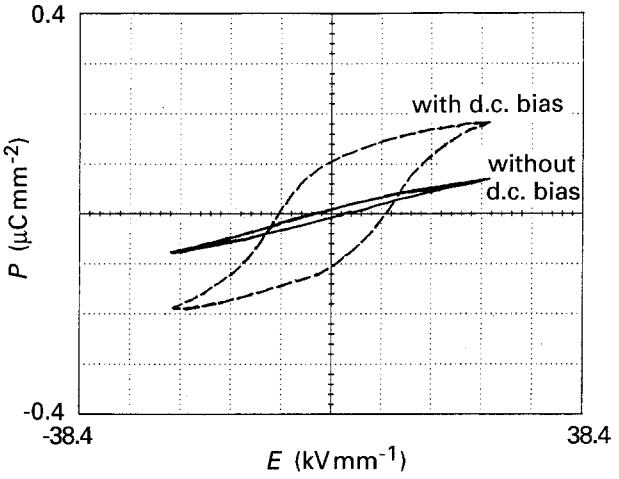

Figure 9 P–E hysteresis loop of a $PbZrO_3$ film with and without a d.c. bias when the alternating field is lower than the AFE→FE transition field.

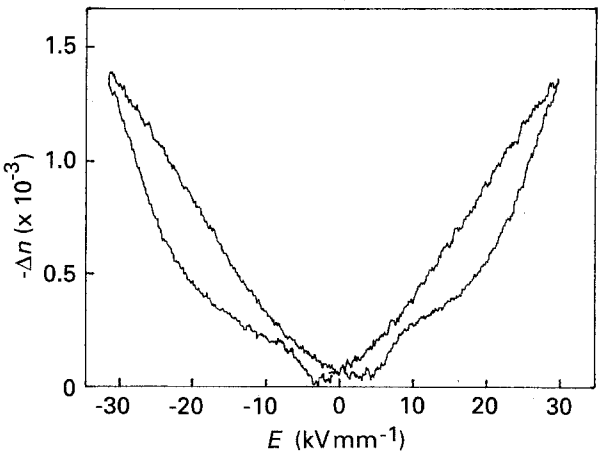

Figure 10 Birefringence shift, Δn, versus electric field, E, plot of an anti-ferroelectric $PbZrO_3$ film on fused SiO_2.

increase in permittivity at the FE→AFE transition was slightly smaller than at the AFE→FE transition.

Weak ferroelectricity was usually observed in these PZ films and was best illustrated in Fig. 8. As the varying d.c. field just completed one half cycle and switched to the negative direction, the permittivity started to increase slightly and then dropped before the AFE→FE transition. A possible ferroelectric interface between the titanium-containing layer and the PZ film might explain this phenomenon; however, earlier results on pure PZ films also showed some ferroelectric behaviour at low fields. This effect will require further detailed study.

Fig. 9 demonstrates the d.c. bias-induced hysteresis behaviour obtained in the antiferroelectric films. As expected, this film behaved like a linear capacitor when the alternating field ($\pm$ 24.6 kV mm^{-1}) was below the AFE→FE transition field ($\sim$32.3 kV mm^{-1}). When biased with a d.c. voltage at 16 V (24.6 kV mm^{-1}), the P–E hysteresis loop behaved like a normal ferroelectric material with two polarization states. This was originated from the hysteresis in the AFE↔FE phase transitions.

The films deposited on fused SiO_2 substrate were electroded with an interdigital pattern having a gap width of 10 μm. The birefringence curve shown in Fig. 10 again showed the ferroelectric behaviour at small fields. The AFE→FE transition was accompanied by a steep increase in the birefringence. A detailed description of this transverse electro-optic behaviour has been given elsewhere [13].

4. Conclusion

AFE $PbZrO_3$ films derived from acetate precursors were deposited on several substrates by an automatic dip-coating process. The phase inhomogeneity observed in these films was attributed to the volatility of the lead species formed during the precursor decomposition process. A thin TiO_2 layer was able to facilitate the formation of the perovskite $PbZrO_3$ and also inhibit the interactions between lead and SiO_2 at the processing temperature. X-ray diffraction revealed the superstructure characteristic of the antiferroelectric phase in these films. The antiferroelectric properties, along with the d.c. bias behaviour, were measured for $PbZrO_3$ films at room temperature.

References

1. E. SAWAGUCHI, G. SHIRANE and Y. TAKAGI, *J. Phys. Soc. Jpn* **6** (1951) 333.
2. G. SHIRANE, E. SAWAGUCHI and Y. TAKAGI, *Phys. Rev.* **84** (1951) 476.
3. E. SAWAGUCHI, H. MANIWA and H. HOSHINA, *ibid.* **83** (1951) 1078.
4. H. FUJISHITA, Y. SHIOZAKI, N. ACHIWA and E. SAWAGUCHI, *J. Phys. Soc. Jpn* **51** (1982) 3583.
5. L. N. CHAPIN and S. A. MYERS, *Mater. Res. Soc. Symp. Proc.* **200** (1990) 153.
6. C.-C. HSUEH and M. L. MECARTNEY, *ibid.* **200** (1990) 219.
7. A. H. CARIM, B. A. TUTTLE, D. H. DOUGHTY and S. L. MARTINEZ, *J. Am. Ceram. Soc.* **74** (1991) 1455.
8. K. D. PRESTON and G. H. HAERTLING, *Integr. Ferroelect.* **1** (1992) 89.
9. S. L. SWARTZ, S. J. BRIGHT, P. J. MELLING and T. R. SHROUT, *Ferroelectrics* **108** (1990) 71.
10. S. HIRANO and K. KATO, *J. Non-Cryst. Solids* **100** (1988) 538.
11. B. JAFFE, *Proc. Inst. Radio Eng.* **49** (1961) 1264.
12. K. UCHINO and S. NOMURA, *Ferroelectrics* **50** (1983) 191.
13. F. WANG, K. K. LI and G. H. HAERTLING, *Opt. Lett.* **17** (1992) 1122.
14. D. BERLINCOURT, H. H. A. KRUEGER and B. JAFFE, *J. Phys. Chem. Solids* **25** (1964) 659.
15. G. H. HAERTLING, *Ferroelectrics* **116** (1991) 51.
16. K. K. LI, G. H. HAERTLING and W.-Y. HOWNG, *Integr. Ferroelect.* **3** (1992) 81.
17. F. WANG, C. B. JUANG, C. BUSTAMANTE and A. Y. WU, in "Proceedings of the 4th International SAMPE Electronic Conference", Albuquerque, New Mexico, June 1990 (Society for the Advancement of Materials and Process Engineers, Covina, CA, 1990) p. 712.
18. Y. TAKAHASHI, Y. MATSUOKA, K. YAMAGUCHI, M. MATSUKI and K. KOBAYASHI, *J. Mater. Sci.* **25** (1990) 3960.
19. K. D. BUDD, S. K. DEY and D. A. PAYNE, *Br. Ceram. Proc.* **36** (1985) 107.
20. Y. TAKAHASHI and K. YAMAGUCHI, *J. Mater. Sci.* **25** (1990) 3950.
21. B. A. TUTTLE, private communication (1992).
22. K. K. LI, G. H. HAERTLING and W.-Y. HWONG, presented at the American Ceramic Society 94th Annual Meeting, Minneapolis, MN, April 1992 (Abstr. 45-E-92)

Received 19 October 1992
and accepted 12 May 1993